LU TP 16-31
June 2016

The ’t Hooft model as a testing ground for Quantum Chromodynamics

Felix Tellander

Department of Astronomy and Theoretical Physics, Lund University

Bachelor thesis supervised by Johan Bijnens

Abstract

We study a 1+1 dimensional Yang-Mills model in the light-cone gauge (the 't Hooft model). The colour group is $SU(N)$ and we study the limit $N \to \infty$, the limit is taken such that g^2N is kept constant. In this limit the only contributing diagrams are planar diagrams without gluon-gluon interactions. Using this, it is shown that there are no free quarks in this model. The bound state wave equation is derived which gives the meson masses and light-cone momentum space wave functions for the model. From this the decay amplitudes are calculated and we show that the model is not integrable and that the pion (massless meson) decouples. We also calculate the form factors which qualitatively show the charge distribution inside the meson.

Populärvetenskaplig introduktion

Allt vi ser är uppbyggt av små partiklar som vi kallar atomer. Men atomerna är inte fundamentala, de består av ännu mindre partiklar och faktiskt, är de mesta av dem tomrum. En atom har liknande struktur som vårt solsystem, det finns en mycket tung kärna i mitten (solen) och lättare elektroner som kretsar runt den (planeterna). Mellan kärnan och elektronerna finns mestadels tomrum, precis som i vårt solsystem. Såvitt vi vet är elektronerna fundamentalpartiklar och består därför inte av något mindre. Kärnan å andra sidan, består av protoner och neutroner och de i sin tur består av något som kallas kvarkar. Den längdskala är på är otroligt liten, radien av en proton är ungefär 10^{-15} meter vilket är av samma storleksordning som om du tar bredden på ett hårstrå och dela upp den i 500 miljoner bitar. Den gren av fysiken som behandlar dessa små partiklar och längder är partikelfysik och det är till detta område som den här uppsatsen tillhör. För att förstå detta arbete måste vi först gå igenom några grundläggande koncept inom partikelfysik.

Om du tar din mobiltelefon och kasta den så kommer den så småningom störta i marken. Den kraft som drar ner telefonen är tyngdkraften. Detta är samma kraft som håller jorden i sin bana runt solen. För att fortsätta vår analogi mellan atomen och solsystemet behöver vi en kraft som håller elektronerna i omloppsbana runt kärnan. Denna kraft är den elektromagnetiska kraften och som uppkommer eftersom elektronerna och kärnan har olika elektrisk laddning. Vi säger att kärnan har positiv laddning och en elektron negativ laddning, elektromagnetism fungerar så att olika laddning attraherar och samma laddningar repellerar. De olika delarna av atomen hålls alltså samman av den elektromagnetiska kraften. Men vi sade att kärnan är sammansatt av ännu mindre partiklar, mest fundamentalt av kvarkarna. Kärnan hålls inte samman av den elektromagnetiska kraften, utan i själva verket finns det så mycket positiv laddning i kärnan att den elektromagnetiska kraften försöker bryta isär den. Kraften som hålla ihop kvarkarna är den starka kraften, den har fått sitt namn eftersom den är den starkaste kraft vi känner till. Liksom för den elektromagnetiska kraften finns det laddningar associerade med denna kraft. Växelverkan mellan kvarkar beskrivs med kvantkromodynamik, QCD, där det finns tre laddningar associerade med den starka kraften: grön. röd och blå.

Den modell vi använder i det här arbetet för att beskriva kvarkarnas växelverkan är 't Hooft-modellen. Denna modell beskriver interaktionerna mellan kvarkarna men med vissa förenklande antaganden jämfört med QCD. I 't Hooft-modellen antar vi att antalet färgladdningar är mycket stort, vi antar faktiskt att det är oändligt. Vi kommer också att anta att det bara finns en rumsdimension, inte tre som i den verkliga världen. Under dessa antaganden har jag beräknat massan av mesoner, dessa är partiklar som består av två kvarkar. Mesoner har totalt ingen elektrisk laddning, men kvarkarna har, och därför studera vi hur den elektriska laddningen är fördelad inuti meson. Ett kvalitativt sätt att studera detta är att beräkna de elektromagnetiska formfaktorerna, dessa är också möjliga att mäta experimentellt. Partiklar som mesoner är i allmänhet inte är stabila utan kommer sönderfalla till andra partiklar. Den tid det tar för dem att sönderfalla och vilka partiklar de sönderfaller till styrs av partiklarna sönderfalls amplituder. Dessa kan, precis som mesonernas massa och formfaktorerna, jämföras med experimentella data.

Acknowledgements

I would like to thank my mentor prof. Johan Bijnens for providing me with this project and for trusting me with much freedom throughout the work.

Felix Tellander

Contents

1 Introduction

Two-dimensional quantum field theories are of interest because they provide insight in non-perturbative aspects of quantum field theory. In a two-dimensional space-time the kinematic is much simplified compared to in four dimensions which have allowed complete solutions for many models involving interacting fields, see the review [1] for examples. A two-dimensional approach to extended QCD proposed by [2] have recently been studied in [3].

In this thesis we will study a two-dimensional model for QCD proposed by 't Hooft in [4, 5]. For this model, which is a 1+1 dimensional Yang-Mills model, our main goal is to derive the bound state wave equation for mesons. Once this is obtained we can calculate other quantities such as decay amplitudes and form factors. The bound state equation is derived from the Bethe-Salpeter equation but in order to use this equation we need to know the dressed fermion propagator. To derive this we need to use the fundamental aspects of the 't Hooft model, these are; we are working in the large-N limit (N is the number of colours) and we are working in the light-cone gauge. Due to this, the only diagrams that contribute to the dressed propagator are the planar diagrams with all gluon lines on the same side of the quark line and without any gluon-gluon interactions. This can be summarized in the Dyson equation. When this is solved something that looks as a constituent quark mass appears in the propagator, this mass may be tachyonic for small current masses. However, the mesons in this model will never be tachyonic [6].

Knowing the light-cone momentum space wave functions we may calculate decay amplitudes and transition form factors for the mesons. By studying the on-shell values of the decay amplitudes, i.e. the values for which the decay is kinematically possible, it is shown that the model is non-integrable and that the massless pion decouples, i.e. no massive particle can decay to the pion.

In the following section the 't Hooft model is reviewed and the bound state meson wave equation is derived. We also argue for the formulas for the decay amplitudes and form factors. Section 3 reviews the numerical method used to solve the wave equation and in section 4 the numerical results for the masses, wave functions, decay amplitudes and form factors are presented. Finally we summarize the work and discuss some prospects in section 5.

2 The 't Hooft model

The 't Hooft model is a 1+1 dimensional Yang-Mills model originally presented in ref. [4] and elaborated in ref. [5]. In this section the theory of the model will be presented and I will derive the underlying equations. The goal is to derive the bound state wave equation for mesons from the Bethe-Salpeter equation. We will start with the Yang-Mills Lagrangian [7, 8]:

$$\mathcal{L} = -\frac{1}{4} G_{\mu\nu i}{}^{j} G^{\mu\nu}{}_{j}{}^{i} + \overline{q}^{ai}(i\gamma^{\mu} D_{\mu} - m_a) q_i^a \tag{2.1}$$

where

$$\begin{aligned} G_{\mu\nu i}{}^{j} &= \partial_\mu A_i{}^{j}{}_{\nu} - \partial_\nu A_i{}^{j}{}_{\mu} + g[A_\mu, A_\nu]_i{}^{j} \\ D_\mu q_i^a &= \partial_\mu q_i^a + g \tilde{A}_i{}^{j}{}_{\mu} q_j^a \\ \tilde{A}_i{}^{j}{}_{\mu}(x) &= A_i{}^{j}{}_{\mu}(x) - \frac{1}{N} \delta_i{}^{j} A^k_{k\mu}(x) = -\tilde{A}^{*i}_{j\mu}(x) \end{aligned}$$

and i, j are indices for the colour group $SU(N)$, a denotes the flavour and g is the coupling constant which in two dimensions has the unit of mass. Here $\tilde{A}_i{}^{j}{}_{\mu}$ is the anti-Hermitian, traceless, gluon field. The Lagrangian in equation (2.1) differs from 't Hooft's original in the sense that the colour group here is $SU(N)$ while 't Hooft used $U(N)$. This difference is not relevant to leading order in $1/N$ [7].

The following results will be derived in the large-N limit in the light-cone gauge (see section 2.1). The limit is implemented as $N \to \infty$; $g^2 N$ constant which means that the only diagrams that contribute to the matrix elements are planar diagrams with no fermion loops and no gluon self-interactions [4]. We take the opportunity here to introduce a new way of writing Feynman diagrams which will focus on the colour flow in the interactions. A quark carries one colour index, see equation (2.1), and will be therefore be represented by a line carrying one index. A gluon carries two indices and will therefore be represented by two lines each carrying one index. This can be written

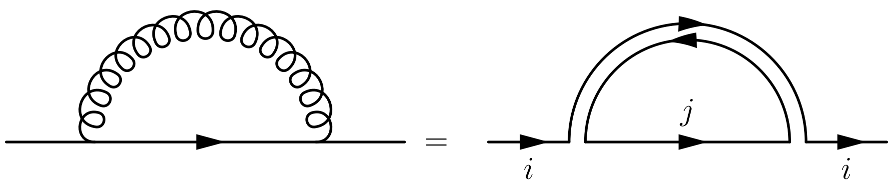

(2.2)

.

Note that the index loop j is independent of the final and initial states so the index j may be chosen freely and the loop will therefore contribute with a factor N in calculation of the matrix elements. Also note that the direction of j changes, this means that it will change from being a lower to an upper index through the loop. To see why certain diagrams' contribution vanishes in the large-N limit, let's study the two following diagrams

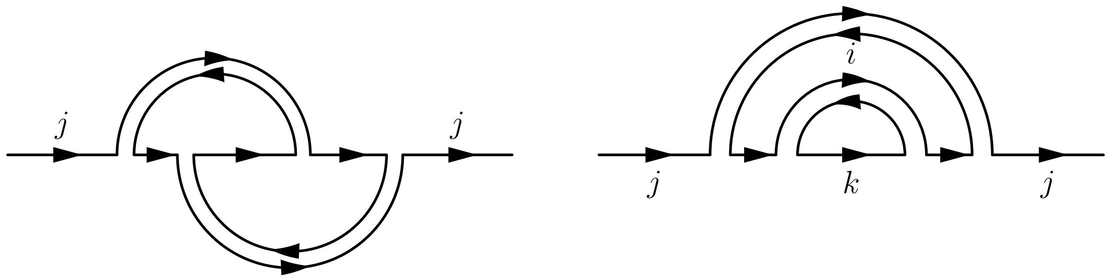

The first diagram has no index loops and hence it contribution goes as $\sim g^4$ (one g for each vertex). We take the limit such that g^2N is kept constant, this means that the first diagram will go as $(g^2N)^2/N^2$, since the numerator is constant the contribution will go to zero as $N \to \infty$. For the second diagram on the other hand, we have two index loops so the diagram will go as $g^4N^2 = (g^2N)^2$ which is kept constant as $N \to \infty$. Therefore, the contribution from the second diagram will not vanish in the large-N limit. In general, the only diagrams that contribute in the large-N limit are the diagrams where all gluon lines are on the same side of the fermion line. This still allows quite complicated diagrams but because of our particular choice of gauge the gluons have no self-interactions making the contributing diagrams simple. It is this insight which makes the derivation of the dressed fermion propagator in section 2.1 and the Dyson equation in section 2.2 so simple.

2.1 Dressed quark propagator

We define the quark propagator as

$$= \frac{i(\not{p} + m)}{p^2 - m^2 + i\epsilon} \tag{2.3}$$

and introduce the notation

$$\tilde{S}(p) = \frac{i(\not{p} + m)}{p^2 - m^2 + i\epsilon}. \tag{2.4}$$

For convenience we introduce the light-cone coordinates. These are obtained by rotating the 1+1 dimensional Minkowski space by $\pi/4$ giving

$$x^{\pm} = \frac{1}{\sqrt{2}} \left(x^0 \pm x^1 \right). \tag{2.5}$$

The metric is $g_{+-} = g_{-+} = 1,\ g_{++} = g_{--} = 0$ and Dirac's gamma matrices satisfy $(\gamma^+)^2 = (\gamma^-)^2 = 0,\ \{\gamma^+, \gamma^-\} = 2$. The theory is ghost free if we impose the light cone gauge;

$$A_- = \frac{1}{\sqrt{2}}(A_0 - A_1) = A^+ = 0 \tag{2.6}$$

and we can now write the quark propagator as

$$\tilde{S}(p) = \frac{i(\gamma^+ p_+ + \gamma^- p_-) + m}{2p_+ p_- - m^2 + i\epsilon}. \tag{2.7}$$

At the interaction vertices $\tilde{S}(p)$ will always be sandwiched between two γ^+ matrices so the only term that survives in the propagator is the term proportional to γ^-. This can be seen by

$$\gamma^+ \begin{pmatrix} 1 \\ \gamma^+ \\ \gamma^- \end{pmatrix} \gamma^+ = \begin{pmatrix} \gamma^+\gamma^+ \\ \gamma^+\gamma^+\gamma^+ \\ \gamma^+\gamma^-\gamma^+ \end{pmatrix} = \begin{pmatrix} 0 \\ 0 \\ (2 - \gamma^-\gamma^+)\gamma^+ \end{pmatrix} = 2\gamma^+ \begin{pmatrix} 0 \\ 0 \\ 1 \end{pmatrix}. \tag{2.8}$$

This means that we can write the propagator simply as

$$\tilde{S}(p) = \frac{ip_-}{2p_+ p_- - m^2 + i\epsilon}. \tag{2.9}$$

The dressed propagator is the sum of all one-particle irreducible diagrams, 1PI,

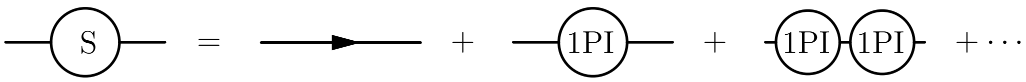

(2.10)

where

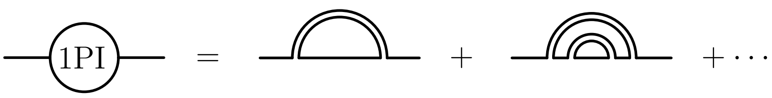

(2.11)

and

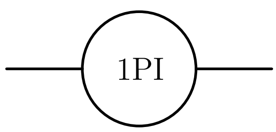

$$= -i\Sigma(p). \tag{2.12}$$

In terms of the 1PI, the dressed propagator, equation (2.10), may be expressed as

$$S(p) = \tilde{S}(p) + \tilde{S}(p)(-i\Sigma(p))\tilde{S}(p) + \cdots \tag{2.13}$$

which is a geometric series with the sum

$$\begin{aligned} S(p) &= \frac{\tilde{S}(p)}{1 + i\Sigma(p)\tilde{S}(p)} = \frac{ip_-/(2p_+p_- - m^2 + i\epsilon)}{1 - \Sigma(p)p_-/(2p_+p_- - m^2 + i\epsilon)} \\ &= \frac{ip_-}{2p_+p_- - m^2 - p_-\Sigma(p) + i\epsilon} \end{aligned} \tag{2.14}$$

2.2 Dyson equation

An explicit expression for Σ can be obtained by solving the Dyson equation

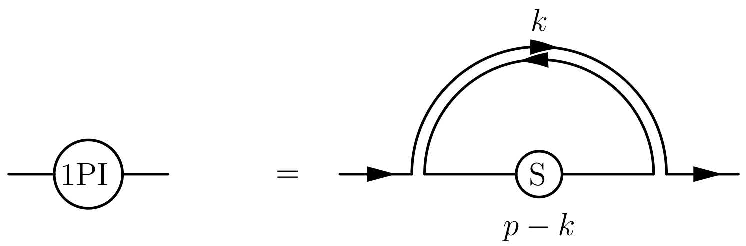

(2.15)

which recursively generates all diagrams in 2.10 and 2.11. The corresponding algebraic expression is

$$\begin{aligned} -i\Sigma(p) &= \int \frac{dk_- d_{k+}}{(2\pi)^2} \frac{i}{k_-^2} S(p-k)(-2ig)^2 \\ &= \frac{-ig^2}{\pi^2} \int dk_- dk_+ \frac{1}{k_-^2} \frac{i(p_- - k_-)}{2(p_+ - k_+)(p_- - k_-) - m^2 - (p_- - k_-)\Sigma(p-k) + i\epsilon}. \end{aligned} \tag{2.16}$$

Note that we can shift $p_+ - k_+ \to -k_+$ so $\Sigma(p)$ must be independent of p_+ and we can therefore write

$$\Sigma(p_-) = \frac{ig^2}{\pi^2} \int dk_- \frac{(p_- - k_-)}{k_-^2} \int dk_+ \frac{1}{-2k_+(p_- - k_-) - m^2 - (p_- - k_-)\Sigma(p_- - k_-) + i\epsilon}. \tag{2.17}$$

The k_+-integral is ultraviolet divergent but a symmetric cut-off will remove the infinity. This integral can directly be evaluated using the Sokhotskyi-Plemelj theorem [9]

$$\left.\begin{aligned} p_- > k_- : &\quad \frac{i\pi}{-2(p_- - k_-)} \\ p_- < k_- : &\quad \frac{-i\pi}{-2(p_- - k_-)} \end{aligned}\right\} = \frac{-i\pi}{2|p_- - k_-|}.$$

Using this, the expression for Σ reduces to

$$\Sigma(p_-) = \frac{ig^2}{\pi^2} \int dk_- \frac{(p_- - k_-)}{k_-^2} \frac{i\pi}{2|p_- - k_-|} = \frac{g^2}{2\pi} \int dk_- \frac{\text{sgn}(p_- - k_-)}{k_-^2}. \tag{2.18}$$

This integral is infrared divergent but since the divergence is not logarithmic as for the previous integral we cannot go around the problem with a symmetric cut-off. However, we will do it anyway, and make the cut-off $\lambda < |k_-| < \infty$ and just postpone the problem with the divergence as $\lambda \to 0$. This is justified since the bound state wave equation, which will be derived in the next section, is independent of λ and therefore we argue that the exact nature of the cut-off will not affect the final result. With the chosen cut-off the integral becomes

$$\begin{aligned}
p_- < -\lambda < 0: \quad & \frac{g^2}{2\pi}\left(\int_{-\infty}^{p_-} \frac{dk_-}{k_-^2} + \int_{p_-}^{-\lambda} \frac{-dk_-}{k_-^2} + \int_{\lambda}^{\infty} \frac{-dk_-}{k_-^2}\right) = \frac{-g^2}{\pi}\left(\frac{1}{p_-} + \frac{1}{\lambda}\right) \\
0 < \lambda < p_-: \quad & \frac{g^2}{2\pi}\left(\int_{-\infty}^{-\lambda} \frac{dk_-}{k_-^2} + \int_{\lambda}^{p_-} \frac{dk_-}{k_-^2} + \int_{p_-}^{\infty} \frac{-dk_-}{k_-^2}\right) = \frac{g^2}{\pi}\left(\frac{1}{\lambda} - \frac{1}{p_-}\right)
\end{aligned}$$

which can be joined together as

$$\Sigma(p_-) = \frac{g^2}{\pi}\left(\frac{\text{sgn}(p_-)}{\lambda} - \frac{1}{p_-}\right). \tag{2.19}$$

By using this expression for Σ the dressed propagator can be written as

$$S(p_-) = \frac{ip_-}{2p_+p_- - M^2 - g^2/\lambda\pi + i\epsilon} \tag{2.20}$$

where we have defined the renormalized quark mass M as

$$M^2 = m^2 - \frac{g^2}{\pi}. \tag{2.21}$$

Because of the cut-off λ the poles of the propagator have been moved to infinity, 't Hooft [5] and Callan *et al.* [7] have argued that this is the reason why there are no free quarks in this model. On the other hand, Einhorn [10] claims that this is wrong and that the confinement is obtained by other means. Nevertheless, everyone agrees on that there are no free quarks in this model, although the underlying reason is somewhat unclear.

2.3 Bethe-Salpeter equation

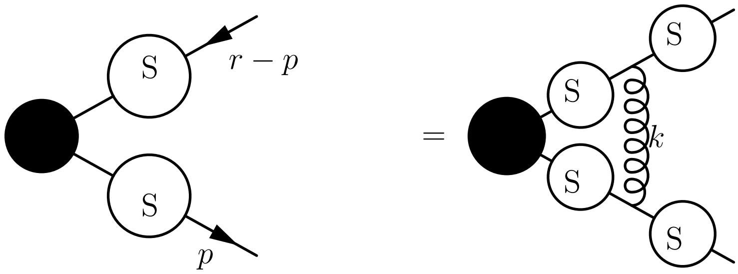

(2.22)

Let $\psi(p, r)$ denote the proper vertex, i.e. the left hand side of the above equation, it is given by

$$\psi(p,r) = \int \frac{dk_- \; dk_+}{(2\pi)^2} \frac{i}{k_-^2} (-2ig)^2 S(p) S(p-r) \psi(p+k, r). \tag{2.23}$$

By integrating both sides with respect to p_+ and defining

$$\phi(p_-, r) = \int dp_+ \; \psi(p_+, p_-, r) \tag{2.24}$$

which is the light-cone momentum space wave function, we obtain

$$\phi(p_-, r) = \frac{-ig^2}{\pi^2} \left(\int dp_+ S(p) S(p-r) \right) \int dk_- \frac{\psi(p_- + k_-, r)}{k_-^2}. \tag{2.25}$$

The p_+−integral can be written in closed form, this is done by a direct implementation of the residue theorem:

$$\begin{aligned}
\int dp_+ S(p) S(p-r) &= \frac{-1}{4} \int dp_+ \frac{1}{p_+ - M_1^2/2p_- - g^2|p_-|/2\lambda\pi p_- + i\epsilon/2p_-} \\
&\cdot \frac{1}{p_+ - r_+ - M_2^2/2(p_- - r_-) - g^2|p_- - r_-|/2\lambda\pi(p_- - r_-) + i\epsilon/2(p_- - r_-)} \\
&= \Big/ \text{ Only non-zero if } p_- \in (0, r_-) \Big/ \\
&= \frac{-2\pi i}{4} \left(r_+ + \frac{M_2^2}{2(p_- - r_-)} + \frac{g^2|p_- - r_-|}{2\lambda\pi(p_- - r_-)} - \frac{M_1^2}{2p_-} - \frac{g^2|p_-|}{2\lambda\pi p_-} \right)^{-1} \\
&= \frac{-i\pi}{2} \left(r_+ - \frac{M_1^2}{2p_-} - \frac{M_2^2}{2(r_- - p_-)} - \frac{g^2}{\lambda\pi} \right)^{-1}
\end{aligned} \tag{2.26}$$

Substituting this into the expression for ϕ yields

$$\phi(p_-, r) = \theta(p_-)\theta(r_- - p_-) \frac{-g^2}{2\pi} \left(r_+ - \frac{M_1^2}{2p_-} - \frac{M_2^2}{2(r_- - p_-)} - \frac{g^2}{\lambda\pi} \right)^{-1} \int dk_- \frac{\phi(p_- + k_-, r)}{k_-^2} \tag{2.27}$$

Taking the k_-−integral with the same cut-off as before gives a principal value integral:

$$\int dk_- \frac{\phi(p_- + k_-, r)}{k_-^2} = \frac{2}{\lambda}\phi(p_-, r) + \mathcal{P} \int dk_- \frac{\phi(p_- + k_-, r)}{k_-^2} \tag{2.28}$$

and substituting this back in the expression gives

$$\begin{aligned}\phi(p_-, r) =& \frac{-g^2}{2\pi} \left(r_+ - \frac{M_1^2}{2p_-} - \frac{M_2^2}{2(r_- - p_-)} - \frac{g^2}{\lambda\pi} \right)^{-1} \\ & \cdot \left(\frac{2}{\lambda}\phi(p_-, r) + \mathcal{P} \int_{p_-}^{r_- - p_-} dk_- \frac{\phi(p_- + k_-, r)}{k_-^2} \right).\end{aligned} \tag{2.29}$$

By simplifying this we note that all dependence on the cut-off parameter λ disappears and the equation can be written as

$$r_+ \phi(p_-, r) = \left(\frac{M_1^2}{2p_-} + \frac{M_2^2}{2(r_- - p_-)} \right) \phi(p_-, r) - \frac{g^2}{2\pi} \mathcal{P} \int_{p_-}^{r_- - p_-} dk_- \frac{\phi(p_- + k_-, r)}{k_-^2}. \tag{2.30}$$

We define new variables

$$\alpha_{1,2} = \frac{\pi M_{1,2}^2}{g^2}, \quad 2r_+ r_- = \frac{g^2}{\pi}\mu^2, \quad x = \frac{p_-}{r_-} \tag{2.31}$$

the final form of the equation becomes

$$\mu^2 \phi(x) = \left(\frac{\alpha_1}{x} + \frac{\alpha_2}{1 - x} \right) \phi(x) - \mathcal{P} \int_0^1 \frac{\phi(y)}{(y - x)^2} dy. \tag{2.32}$$

This is an eigenvalue equation where μ is the mass of the meson consisting of a quark with mass α_1 and an anti-quark with mass α_2, all masses are in units of $g/\sqrt{\pi}$. For this to fit with standard meson phenomenology we put $\pi g^2 = 1$ GeV^2 [7]. This makes it possible to express the mass of the meson and quarks in natural units and hence makes it possible to compare calculations in this model with experimental results.

2.4 Form factors

In this section we consider the electromagnetic transition form factors, the results presented here are fully derived in e.g. [10, 11]. The form factor is defined as

$$F_\mu^{nm} = \langle n | J_\mu | m \rangle \tag{2.33}$$

where J_μ describes the coupling of the meson to the photon. If the meson consists of quark a and anti-quark $\bar{b}$, let ψ^{ab} denote the vertex used in equation (2.23) and let ψ^a denote the vertex of quark a and a photon. For a meson with momentum p, interacting with a virtual photon with momentum q and leaving with momentum p', the minus component of the form factor for quark a is

$$F_-^{a,nm} = \frac{-i2e_a}{\pi} \int d^2k \ \psi_n^{ab}(k,p) S^a(k) \psi^a(k,p) S^a(k-q) \psi_m^{ab}(k-q,p') S^b(k-q). \qquad (2.34)$$

Adding this to $F_-^{b,nm}$ gives us

$$\begin{aligned} F_-^{nm} \ \propto \ & (1-x) \left\{ \int_0^1 dz \ \phi_n[x+(1-x)z]\phi_m(z) \right. \\ & \left. + x^2 \int_0^1 \int_0^1 du \ dz \frac{\phi_n(xu) - \phi_n(x+(1-x)z)}{[x(1-u)+(1-x)z]^2} G(u;q^2)\phi_m(z) \right\} \end{aligned} \qquad (2.35)$$

where

$$\mu_n^2 = \frac{q^2}{x} + \frac{\mu_m^2}{1-x}, \quad G(u;q^2) = \sum_n \frac{\phi_n(u) \int_0^1 \phi_n(v) \ dv}{q^2 - \mu_n^2 + i\epsilon}. \qquad (2.36)$$

2.5 Decay amplitudes

A formal derivation of the decay amplitudes in this model can be found in [7, 11] here I will just present the formulas. Denote the amplitude for the decay $\phi_i \to \phi_{f_1} + \phi_{f_2}$ with $\mathcal{A}(i, f_1, f_2; \omega)$ where ω is a kinematic parameter, the amplitude is given by

$$\begin{aligned} \mathcal{A}(i, f_1, f_2; \omega) \ = & \frac{1}{1-\omega} \int_0^\omega dx \ \phi_i(x) \phi_{f_1}\left(\frac{x}{\omega}\right) \Phi_{f_2}\left(\frac{x-\omega}{1-\omega}\right) \\ & - \frac{1}{\omega} \int_\omega^1 dx \ \phi_i(x) \Phi_{f_1}\left(\frac{x}{\omega}\right) \phi_{f_2}\left(\frac{x-\omega}{1-\omega}\right) \end{aligned} \qquad (2.37)$$

where

$$\Phi(x) = \int_0^1 dy \frac{\phi(y)}{(x-y)^2}. \qquad (2.38)$$

Pair production is only possible if $\mu_i \geq \mu_{f_1} + \mu_{f_2}$ and in this case the on-shell values of ω are [12]

$$\omega_\pm = \frac{\mu_i^2 + \mu_{f_1}^2 - \mu_{f_2}^2 \mp \sqrt{(\mu_i^2 + \mu_{f_2}^2 - \mu_{f_1}^2)^2 - 4\mu_i^2 \mu_{f_2}^2}}{2\mu_i^2} \qquad (2.39)$$

where ω_+ (ω_-) corresponds to the state f_1 moves to the right (left). The initial meson consists of one quark and one anti-quark, the quark goes to the ϕ_{f_2} state and the anti-quark to ϕ_{f_1}.

3 Numerical consideration

Equation (2.32) is solved by using a sine-series anzats. If we change the variables to $x = \frac{1}{2}(1 - \cos\theta)$ and $y = \frac{1}{2}(1 - \cos\theta')$ and put

$$\phi(\theta) = \sum_n \sin(n\theta) \tag{3.40}$$

we obtain

$$\sum_n a_n \mu^2 \sin(n\theta) = \sum_n \left[2a_n \left(\frac{\alpha_1}{1 - \cos\theta} + \frac{\alpha_2}{1 + \cos\theta} \right) \sin(n\theta) + 2\pi a_n n \frac{\sin(n\theta)}{\sin\theta} \right]. \tag{3.41}$$

Multiplying this equation with $\sin(m\theta)$ and integrating over θ and summing over m gives

$$a_m \mu^2 = \sum_n \left[4a_m(\alpha_1 \min\{n, m\} + \alpha_2 (-1)^{n+m} \cdot \min\{n, m\} + nI_{nm}) \right] \tag{3.42}$$

where

$$I_{nm} = \int_0^\pi \frac{\sin(n\theta)\sin(m\theta)}{\sin\theta}. \tag{3.43}$$

Equation (3.42) is a standard matrix eigenvalue problem and can be solved by standard routines in e.g. MATLAB.

The problem with this method is that we enforce the boundary condition $\phi(x = 0) = \phi(x = 1) = 0$. As seen in figure 1 this is not always good and therefore we need many sine-terms to get reasonable approximations. As fast as the wave function begin to oscillate the approximation becomes better. For the massless pion, which is analytically solvable, with eigenvalue and normalized wave function;

$$\mu^2 = 0, \qquad \phi(x) = 1 \tag{3.44}$$

the numerical solutions are exceptionally bad. In figure 1a we see small oscillations even though 1500 terms have been used. It is understandable that this case is difficult because we are trying to approximate a constant (non-zero) line with something that oscillates around 0. Better solutions can be obtained by using adaptive spline methods [12].

4 Numerical results

The results are divided into three sections. In the first section I present the bound state meson wave functions and masses for some different combination of quarks. In the next section I show the form factors for the meson corresponding to the $c\bar{c}-$bound state in the standard model. Finally the decay amplitudes are calculated for the corresponding $c\bar{c}-$bound state and for the massless meson (pion). In this section it is shown that massless two-dimensional QCD is non-integrable and that the pion decouples.

4.1 Wave functions and masses

The wave functions and meson masses are calculated for three different combinations of quarks: both quarks are massless, $m_a = m_b = 0$, a mimic of the $c\bar{c}-$bound state, $m_a = m_b = 1.275$ GeV and what would correspond to the $D^{\pm}-$mesons, $m_a = 1.275$ GeV and $m_b = 2.3$ MeV. The ten first bound state masses for each combination of quarks are shown in table 1. For each meson the four first bound state wave functions are shown in figure 1, 2 and 3.

4.2 Form factors

In figure 4 four different form factors for the $c\bar{c}-$bound state are shown. These are shown as functions of the variable x, which satisfies the following equation

$$\mu_n^2 = \frac{q^2}{x} + \frac{\mu_m^2}{1-x}. \tag{4.45}$$

By re-arranging this we obtain an expression for $-q^2$ and observe that for x between 0 and 1; $-q^2$ has values between 0 and infinity. We may therefore regard $F_-^{nm} = F_-^{nm}(-q^2)$ with $-q^2 \in [0, \infty)$ which might be more familiar to the reader. In figure 5 the form factors F_-^{11} and F_-^{22} are shown as functions or $-q^2$ together with $1/(-q^2)$. We see that both form factors goes to zero as $-q^2 \to \infty$, and it seams reasonable to say that $F \sim 1/(-q^2)$ for large $-q^2$.

4.3 Decay amplitudes

The decay amplitudes are calculated by the expression in equation (2.37) and the on-shell values for the parameter ω are given by equation (2.39). In figure 6 four decay amplitudes for the massless case, $m_a = m_b = 0$, are shown, in these graphs the green marks show the on-shell values of ω. What we want to show here is the difference between figure 6a, 6d and 6b, 6c. The first two are the decay amplitudes $\mathcal{A}(5,1,1)$ and $\mathcal{A}(10,4,1)$ which both contains at least one pion. The figures show that the on-shell amplitudes for decay into a pion is zero which means that the pion decouples. On the other hand, when both final states are massive, the on-shell amplitudes are non-zero as shown in figure 6b and 6c.

Table 1: The bound state masses for the three studied mesons. In the first column the bound state masses for two massless quarks are shown. In the second column the $c\bar{c}-$bound state with bare $c-$quark mass 1.275 GeV is shown and in the third column the bound state of bare quark masses 1.275 GeV and 2.3 MeV is shown.

	Massless	$c\bar{c}$	$D^{\pm}$
m_1	0.00	2.76	1.52
m_2	0.77	3.10	1.99
m_3	1.20	3.33	2.31
m_4	1.53	3.55	2.58
m_5	1.81	3.73	2.81
m_6	2.06	3.90	3.01
m_7	2.28	4.06	3.20
m_8	2.48	4.21	3.37
m_9	2.67	4.36	3.54
m_{10}	2.84	4.49	3.69

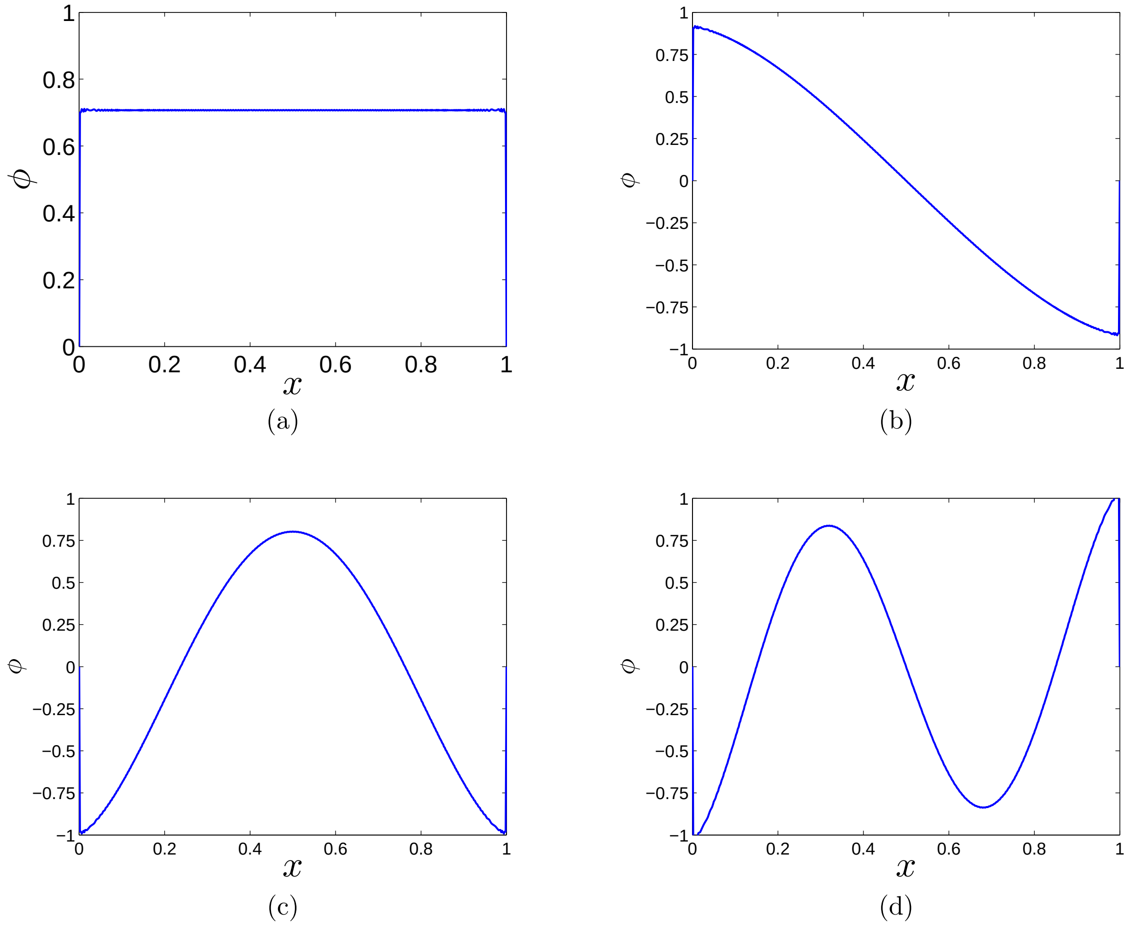

Figure 1: The four first wave functions in the massless case, $m_a = m_b = 0$.

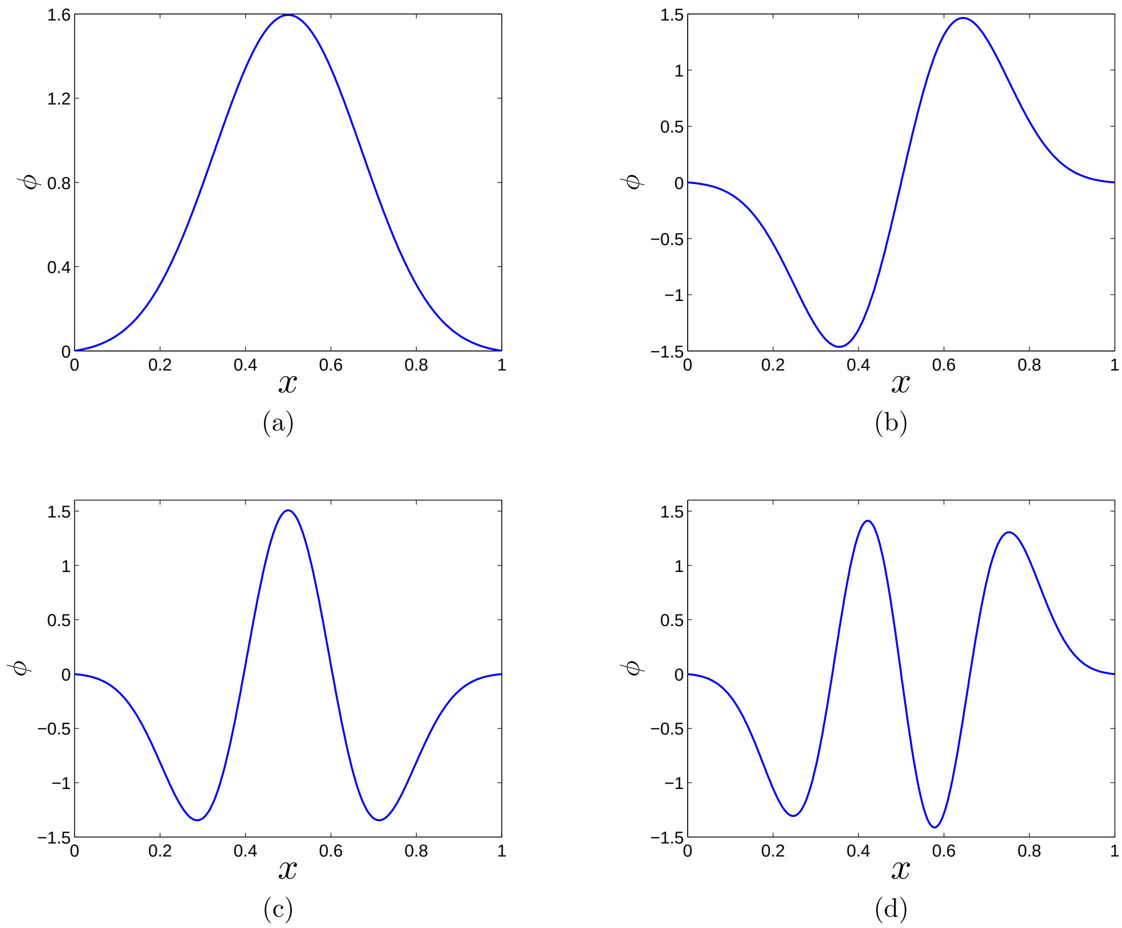

Figure 2: The four first wave functions for the case where we have mimicked the $c\bar{c}$ bound state, i.e. $m_a = m_b = 1.275$ GeV.

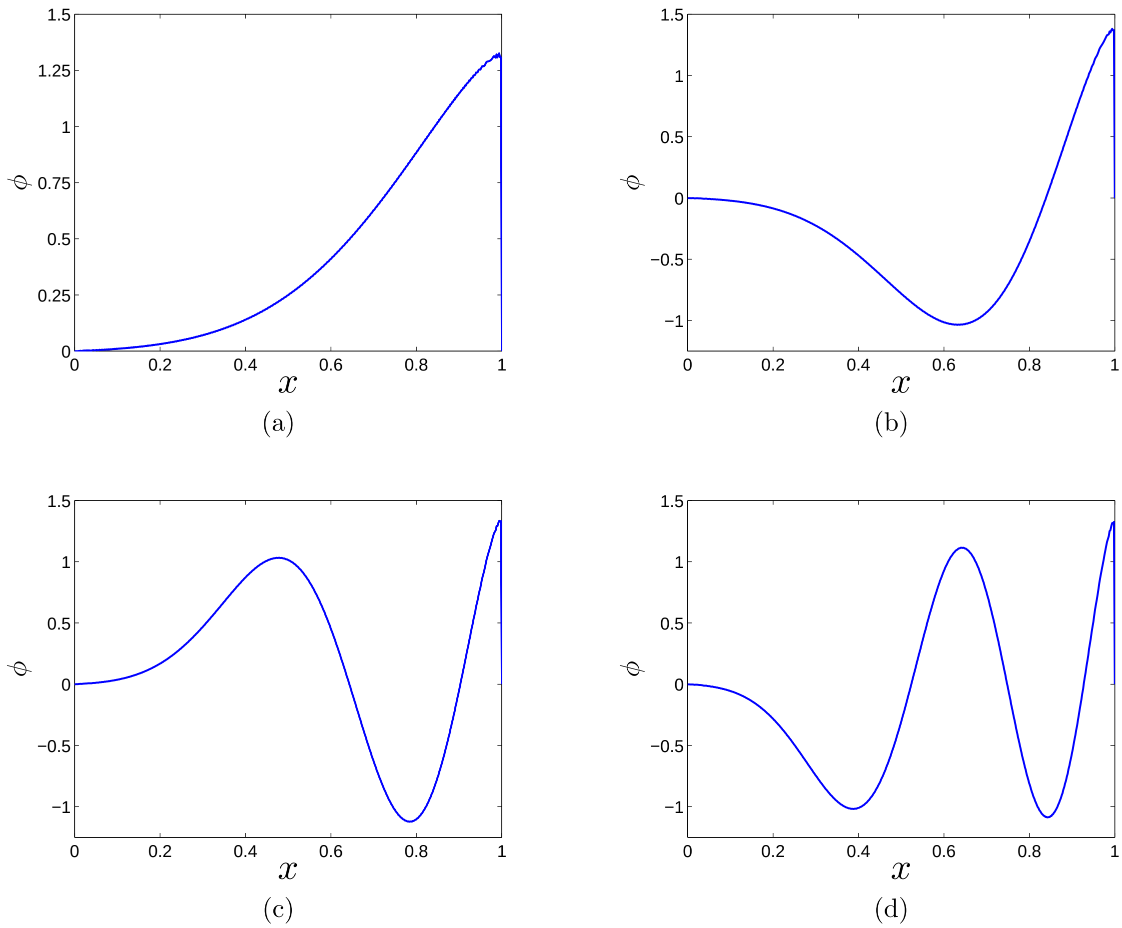

Figure 3: The four first wave functions when the D^+ meson is mimicked, i.e. $m_a = 1.275$ GeV and $m_b = 2.3$ MeV. The wave functions for D^- look the same but mirrored over $x = 0.5$.

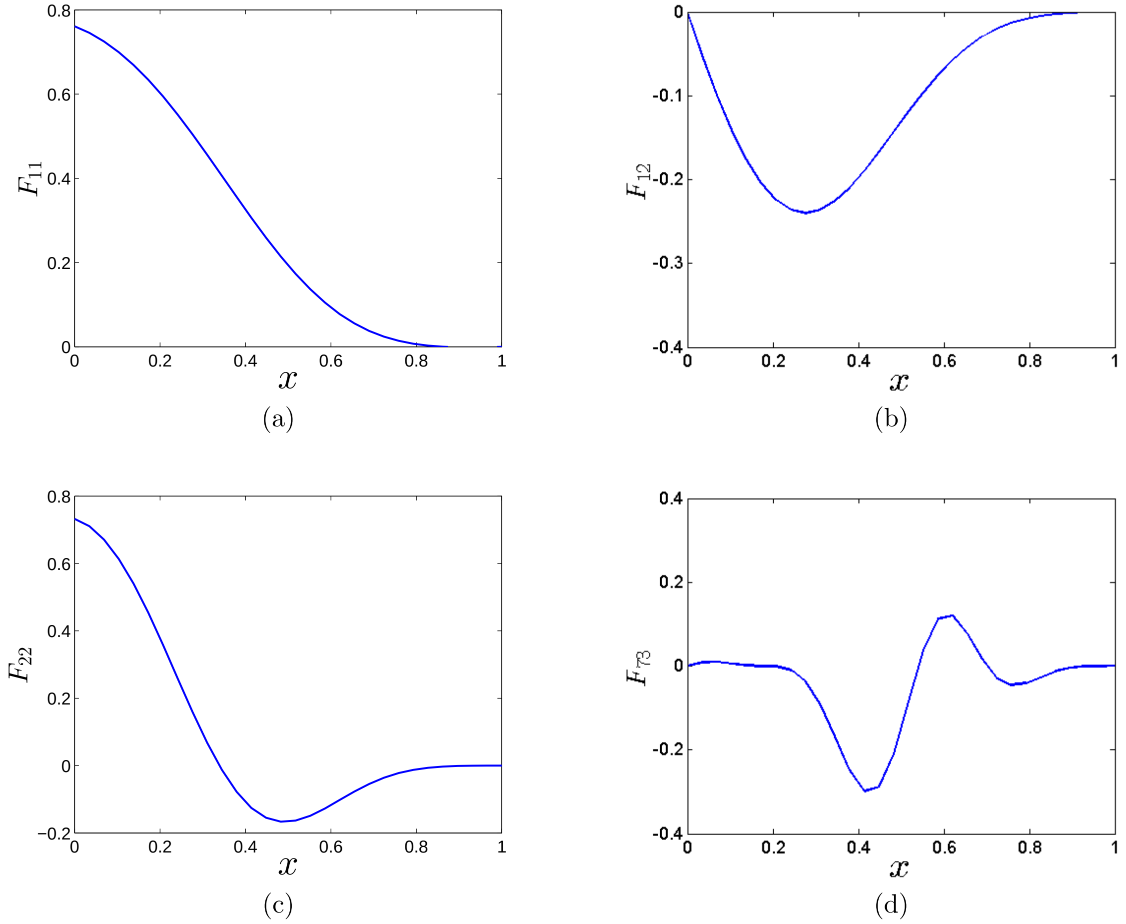

Figure 4: Form factors for the $c\bar{c}$−bound state.

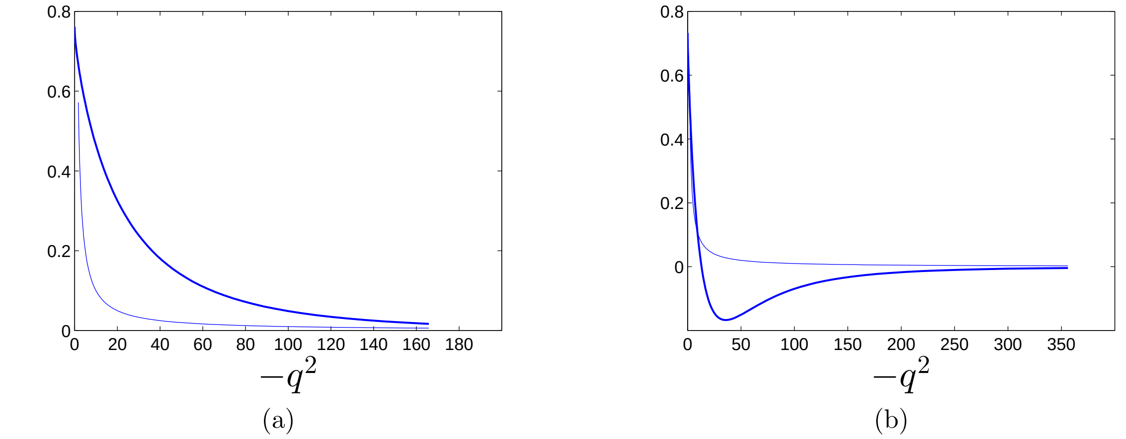

Figure 5: The F_{-}^{11} and F_{-}^{22} form factors (bold lines) for the $c\bar{c}$ bound state as a function of $-q^2$ together with $1/(-q^2)$ (thin line). Note that the form factors approaches zero as $-q^2 \to \infty$.

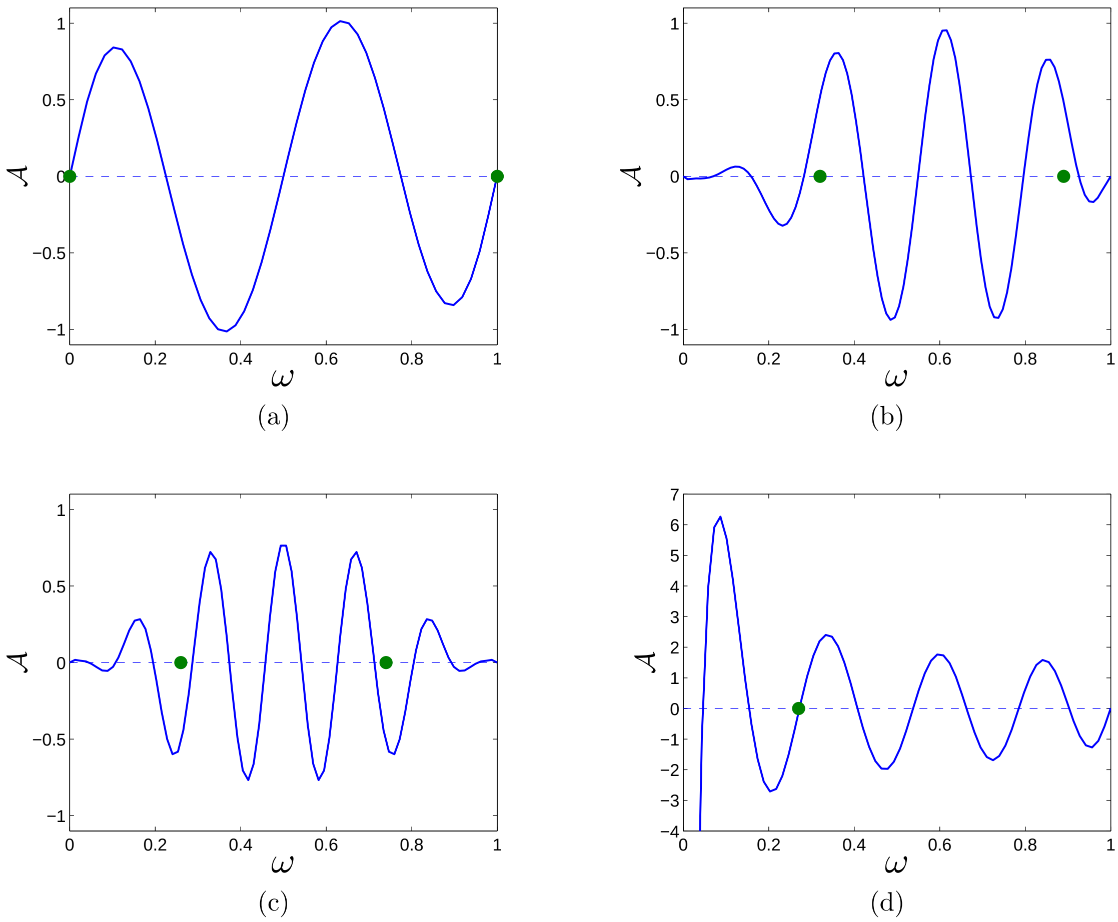

Figure 6: Four decay amplitudes in the massless case, $m_a = m_b = 0$, the green dots mark the on-shell values of ω. In (a) $\phi_5 \to \phi_1 + \phi_1$ is shown and in (b), (c) and (d) $\phi_{10} \to \phi_4 + \phi_2$, $\phi_{14} \to \phi_4 + \phi_4$ and $\phi_{10} \to \phi_4 + \phi_1$ are shown respectively.

This shows that the theory is not integrable, these results are consistent with the results obtained in [12, 13].

In figure 7 the amplitudes for the decay $c\bar{c} \to D^+ + D^-$ are shown. A difference here, which can be seen in table 1, compared to the experimental results is that the $D^\pm-$threshold lies between the first and second state of the $c\bar{c}-$bound state while experimentally it is between the second and third. That is why $\mathcal{A}(1,1,1)$ is not shown in figure 7, it is not allowed.

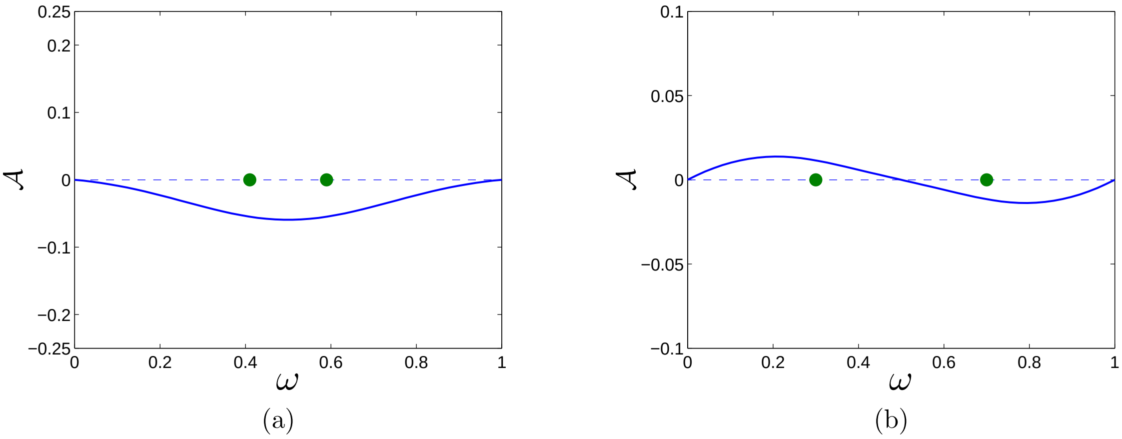

Figure 7: Amplitudes for the $c\bar{c}-$bound state, $m_a = m_b = 1.275$ GeV, decaying into the ground states of $D^{\pm}$. The decay $\phi_2 \to \phi_1 + \phi_1$ is shown in (a) and $\phi_3 \to \phi_1 + \phi_1$ in (b).

5 Summary and prospects

In this thesis we study the masses, wave functions, form factors and decay amplitudes for mesons in the 't Hooft model. This model is a 1+1 dimensional Yang-Mills theory with colour group $SU(N)$ in the light-cone gauge in the limit $N \to \infty$; g^2N constant. In this model the dressed quark propagator is derived to be

$$S(p_-) = \frac{ip_-}{2p_+p_- - M^2 - g^2/\lambda\pi + i\epsilon}, \quad M^2 = m^2 - \frac{g^2}{\pi}.$$

The poles of the propagator are pushed to infinity which means that there are no free quarks in this model, i.e. the 't Hooft model admits confinement. From the Bethe-Salpeter equation a bound state equation for mesons are derived:

$$\mu^2\phi(x) = \left(\frac{\alpha_1}{x} + \frac{\alpha_2}{1-x}\right)\phi(x) - \mathcal{P}\int_0^1 \frac{\phi(y)}{(y-x)^2}dy.$$

where μ are the meson masses in units of $g/\sqrt{\pi}$ and ϕ the wave functions. Using these wave functions the decay amplitudes and form factors are calculated.

It is shown that the decay amplitude is in general non-zero which means that the model is non-integrable. But if one of the final states in the decay is the massless pion, the amplitude is zero which means that the pion decouples. The form factors seems to asymptotically go as $1/(-q^2)$ which is expected from perturbative QCD.

The bound state wave equation is a hyper singular integral equation making the numerical solutions very unstable. However, great accuracy and stability have been obtained in [12] by using an adaptive spline method. Further work could include a deeper study of the form factors especially associated with the pole expansion used in e.g. [11].

References

[1] E. Abdalla, Two-dimensional quantum field theory, examples and applications.
URL http://arxiv.org/abs/hep-th/9704192

[2] D. B. Kaplan, Extended qcd.
URL http://arxiv.org/abs/1306.5818

[3] F. Hidenori, Y. Ryo, Renormalization of extended qcd2., Progress of Theoretical Experimental Physics: PTEP (10) (2015) 1.

[4] G. 't Hooft, A two-dimensional model for mesons., Nuclear Physics, Section B 75 (3) (1974) 461–470.

[5] G. 't Hooft, A planar diagram theory for strong interactions., Nuclear Physics, Section B 72 (3) (1974) 461–473.

[6] S. Coleman, 1/n, The 1979 International School of Subnuclear Physics: Pointlike Structures Inside and Outside Hadrons.
URL http://slac.stanford.edu/pubs/slacpubs/2250/slac-pub-2484.pdf

[7] J. Callan, C.G., N. Coote, D. Gross, Two-dimensional yang-mills theory: A model of quark confinement., Physical Review D (Particles and Fields) 13 (6) (1976) 1649 – 1669.

[8] M. E. Peskin, D. V. Schroeder, An introduction to quantum field theory., Reading, Mass. : Addison-Wesley, cop. 1995, 1995.

[9] E. B. Saff, A. D. Snider, Fundamentals of complex analysis for mathematics, science, and engineering., Englewood Cliffs, N.J. : Prentice-Hall, cop. 1976, 1976.

[10] M. Einhorn, Confinement, form factors, and deep-inelastic scattering in two-dimensional quantum chromodynamics., Physical Review D 14 (12) (1976) 3451–3471.

[11] R. Jaffe, P. Mende, When is field theory effective?., Nuclear Physics B B369 (1) (1992) 189 – 218.

[12] W. Krauth, M. Staudacher, Non-integrability of two-dimensional qcd.

[13] E. Abdalla, R. Mohayaee, Decay amplitudes in two-dimensional qcd., Physical Review D 57 (6) (1998) 3777 – 3785.